Accumulator for the production of intense positron pulses

D. B. Cassidy and S. H. M. Deng
Department of Physics and Astronomy, University of California, Riverside, California 92507

R. G. Greaves
First Point Scientific, Inc., Agoura Hills, California 91301

A. P. Mills, Jr.
Department of Physics and Astronomy, University of California, Riverside, California 92507

(Received 11 April 2006; accepted 17 June 2006; published online 19 July 2006)

An intense pulsed positron source has been developed using a buffer gas trap to accumulate large numbers of positrons and create a dense plasma, which may then be bunched and spatially focused. Areal densities of more than 3×10^{10} e^+ cm^{-2} have been achieved in a subnanosecond pulse producing an instantaneous positron current of more than 10 mA. We describe various aspects of the device including a detection technique specifically developed for use with intense positron pulses. Two applications are also described as well as future experiments such as the formation of positronium molecules and the positronium Bose-Einstein condensate. © *2006 American Institute of Physics.* [DOI: 10.1063/1.2221509]

I. INTRODUCTION

Even now, more than 70 years after the prediction[1] and subsequent observation[2] of the positron, these antiparticles remain somewhat elusive to experimenters wishing to create and utilize them in large numbers. Nevertheless, much progress has been made, particularly in the creation of slow positron beams derived from radioactive sources. Indeed, the first moderated slow positron beams of a half-century ago[3–5] had intensities of only a few positrons/s. The state of the art for such beams has steadily improved[6] and it is now possible to produce source-based beams with more than 10^7 e^+ s^{-1}.[7]

It is also possible to produce more intense beams; one way is by creating positron-emitting isotopes external to the beamline (but in an associated facility) using a nuclear reactor[8] or *in situ* with a deuteron or proton accelerator.[9] Alternatively, intense beams may be created via pair production using a high-energy electron linac.[10] However, such arrangements are generally very expensive and it is not often possible to justify such expense merely for the generation of a positron beam, particularly since such beams have so far been limited to intensities less than $\sim10^9$ e^+ s^{-1}. In fact, achieving a beam with 10^{10} e^+ s^{-1} seems to be something of a design goal for intense slow beams.[11] Furthermore, many experiments that would certainly benefit from these intense beams can, in fact, be performed successfully with lower intensity source based beams and a little ingenuity.[12] Thus, the vast majority of positron beams built so far have been derived from commercially supplied radioisotope sources, ^{22}Na being the material of choice.[13]

Developments in positron trapping technology[14] over the last decade or so have, for certain types of experiments at least, mitigated the need for intense positron beams. That is, while it is still desirable to have the most intense primary beam possible, by accumulating positrons for a long time one may produce high quality pulsed or dc beams[15] or very intense positron bursts[16] even with rather modest primary beams. Positron traps were also crucial in creating the first low energy antihydrogen atoms,[17] and have been used for groundbreaking investigations of positron-matter interactions.[18]

Partly as a consequence of the limited positron beam intensities, there have been almost no experimental studies of high density positronium (Ps) systems, and the apparatus we describe here has been used to perform the first measurements of interacting positronium atoms.[16] The ultimate goal of our research is the creation and study of the positronium Bose-Einstein condensate (BEC).[19] However, as we progress towards this admittedly ambitious objective, we intend to complete a number of additional experiments including the creation and observation of the dipositronium molecule[20] and studies of time dependent defect density fluctuations in thin films induced by intense laser pulses.[21]

In this article, we describe the operation of a positron accumulator that incorporates a number of well-known techniques for the collection and manipulation of positrons. Although the goal of a Ps BEC is still some way in the future, many of the characteristics of the primary positron beam required to achieve this[22] have already been realized, and we outline these and discuss future improvements. We also describe some supplemental techniques developed for measuring single shot positronium lifetimes and present data that highlight the capabilities of the device.

II. APPARATUS

A. Overview

The positron accumulator is based on the buffer gas system developed by Murphy and Surko.[23] The system is slightly different from the usual Surko-type traps in that the accumulation and trapping stages are decoupled in the same manner as described by Greaves and Moxom.[24] This leads to

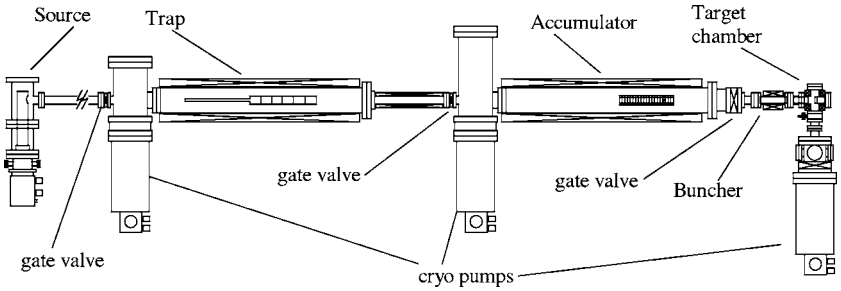

FIG. 1. Layout of the instrument. A slow positron beam containing $\sim 6\times 10^6$ s^{-1} is generated in the source chamber and then enters a two-stage Surko-type buffer gas trap which generates pulses of 3×10^5 positrons and delivers them to the accumulator at a repetition rate of 4 Hz. These pulses are then transferred to the accumulator where they form a well-defined plasma which is compressed in the accumulator before being sent into a buncher, from which emerges a subnanosecond pulse. The total length of the system is ~5.5 m.

a modular system comprising a slow positron beam, a trap, an accumulator, and a target chamber. Each of these sections is essentially an independent experimental system, although obviously the operation of each section is entirely contingent on that of its predecessor. A schematic of the entire experimental layout is shown in Fig. 1. An axial magnetic field confines the positrons radially, and various electrostatic potentials are applied to define the different moderation, trapping, accumulation, bunching, and acceleration sections required for producing intense nanosecond pulses. All pumps used throughout the system were oil-free to avoid the possibility of hydrocarbons with high positron annihilation cross sections[25] compromising the positron lifetime in the accumulator.

B. Source and trap

Positrons from a 25 mCi ^{22}Na source were moderated with a solid neon moderator[26] to generate the slow positron beam used in this work. Moderators are usually grown at a temperature of 7 K with ultrapure (99.999%) neon admitted at a pressure of 1×10^{-4} Torr for 7 min. We have found that higher efficiencies are obtained if the system is pumped during moderator growth, as opposed to simply filling the chamber with gas. Typically we obtain beam intensities greater than 6×10^6 e^+ s^{-1} with a new moderator, but exposure to N_2 buffer gas from the trap generally causes a relatively rapid reduction to $\sim 4\times 10^6$ e^+ s^{-1}. Following this initial decline, and with continuous exposure to the buffer gas, our moderator efficiency generally decays by around 5% per day. Moderators that are not exposed to the buffer gas usually decay by less than 2% per day, with no initial drop. Further reduction of the conductance between the source and the trap should help maintain moderator integrity.

As mentioned above, the device described here is slightly different from the usual Surko-type traps in which a three-stage electrode structure is usually fully enclosed in a single, differentially pumped, vacuum system. Here the trap and accumulator sections together (see Fig. 1) constitute a decoupled Surko trap, wherein the accumulator is equivalent to the third stage where positrons are eventually stored.

The main reason for this is simply to provide a better vacuum environment for the positrons and thus longer lifetimes, although this design also obviates the need for expensive large-bore magnets and vacuum chambers, hence reducing the cost of the device. Transferring the positron output from a buffer gas trap to an UHV environment has also been used to prepare positron plasmas for antihydrogen formation experiments.[27]

Figure 2 shows the electrode structure of the trap section. A buffer gas is introduced into stage 1, where the narrow electrode diameter [8 mm inside diameter (i.d.)] permits a high-pressure region to be maintained by differential pumping. This ensures a high probability of a positron-molecule collision occurring in a single pass through the trap, thus permitting high trapping efficiency. The interelectrode potential differences are tuned to maximize the probability of an electronic excitation of nitrogen close to the threshold energy (~8.8 eV). This is currently the most efficient collision process known for trapping positrons because of its large cross section.[28]

Although the potential structure divides the trap into three distinct stages, the buffer gas pressure gradient between the second and third stages (referred to here as stages "2a" and "2b," respectively) is minimal and as a result the system cannot be operated as a true three-stage trap. With only two effective stages of differential pumping in the trap and the concurrently higher pressure in the "third stage" (2b) the positron lifetime is greatly reduced in comparison with a true three-stage trap, and we find typical lifetimes of approximately 0.3 s, mainly due to transport of positrons across the magnetic field.[29] The base pressure in the trap chamber is 1×10^{-10} Torr, which increases to $\sim 5\times 10^{-6}$ Torr when the buffer gas is introduced. However, the pressure inside stage 1 is approximately 1×10^{-3} Torr and about one order of magnitude less in stage 2.

Stage 2b contains a segmented electrode to allow for the application of a quadrupole "rotating wall" (RW) electric field, which is used to compress the positrons radially after they have been captured.[30,31] The eight-segmented electrode to which the rf signal is applied constitutes half of the length

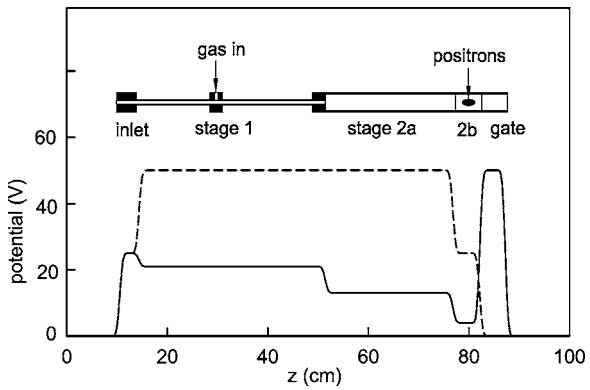

FIG. 2. Above: scaled drawing of the trap electrode structure. Below: the axial potential profiles for trapping (solid line) and releasing ("dumping") positrons (dashed line).

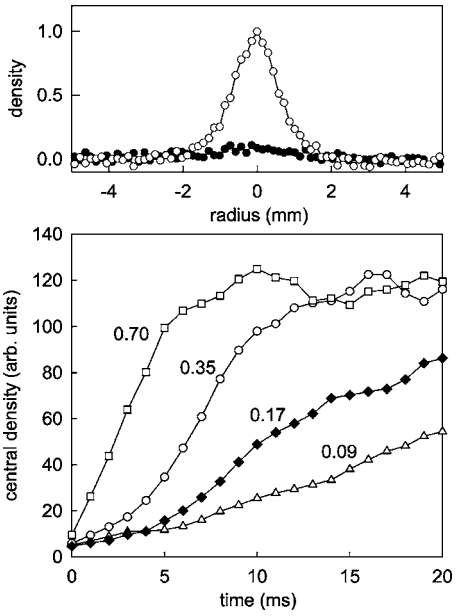

FIG. 3. Above: radial profiles of positrons in the trapping section. (●) without rf applied; (○) with rf applied. Below: central density of the positron cloud as a function of time for various values of applied rf signal amplitude, shown in the figure in volts. The rf was switched on at $t=0$.

of stage 2b. The i.d. of these electrodes is 2.54 cm. With this addition, we measure lifetimes of around 2 s (limited by annihilation) and the trapping efficiency is almost doubled to approximately 20% because losses from radial transport are effectively eliminated. Because of the relatively short lifetime, the trap is typically operated at a repetition rate of 4 Hz in order to maximize the trap throughput. Other groups are also developing two-stage Surko-type traps for applications requiring high quality pulsed positron beams with pulse repetition frequencies >1 Hz.[32]

The effectiveness of the compression is shown in Fig. 3. The upper panel shows the positron radial profiles with and without the rotating wall applied, indicating a positron cloud with a final diameter of about 1.3 mm full width at half maximum (FWHM). The rf was 5 MHz. These profiles were obtained by imaging positrons dumped onto a phosphor screen. The lower panel shows the central density as a function of time for various amplitudes of applied frequency. This figure illustrates that very rapid compression can be obtained, with central density doubling times of only a few milliseconds, in contrast to the time scales of seconds reported for compression in the plasma regime.[31]

Figure 4 shows the trap efficiency as a function of applied rf and amplitude. A NaI scintillator attached to a photomultiplier was placed just after the trap with the gate valve to the accumulator closed, and the anode signal was recorded directly with a digital storage oscilloscope that was triggered by the trap dump pulse. As is evident from the figure, we find that for low applied rf amplitudes, compression is centered on a single, well-defined frequency, which we have identified as the axial bounce frequency. As the rf amplitude is increased, the compression becomes broadband in character below the bounce frequency. In order for the rotating wall to be effective it was necessary to introduce a cooling gas (in this case, SF_6) at a pressure approximately one-fifth that of

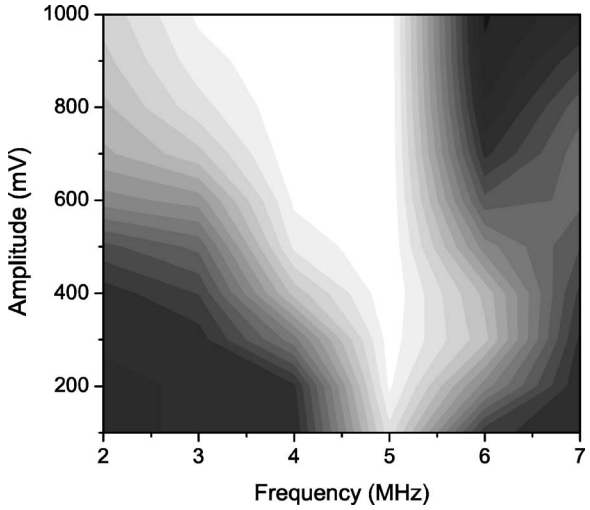

FIG. 4. Amplitude-frequency scan of trapping efficiency for the rf signal applied to the rotating wall electrode in the trap. The color shade indicates the efficiency, with white corresponding to the maximum value of approximately 20%.

the buffer gas. The effect of the extra gas on the lifetime was not significant when the rotating wall was switched off. During normal trap operation the rotating wall is always on.

It should be noted that the compression effect described here is somewhat different from the usual application of the rotating wall technique, in which plasma modes are excited. With less than 200 000 positrons per pulse in the trap the positrons are not in a well-defined plasma state. Indeed, even for much smaller numbers of positrons ($<10^4$) compression is achieved, suggesting that the rotating wall in this configuration is operating according to a different principle that is usually thought to be the case. Further studies are under way to elucidate the mechanism.

C. Positron accumulator

The electrode structure of the accumulator and the typical operating potential profiles are shown in Fig. 5. As can be seen from this figure, the trap contains a harmonic potential

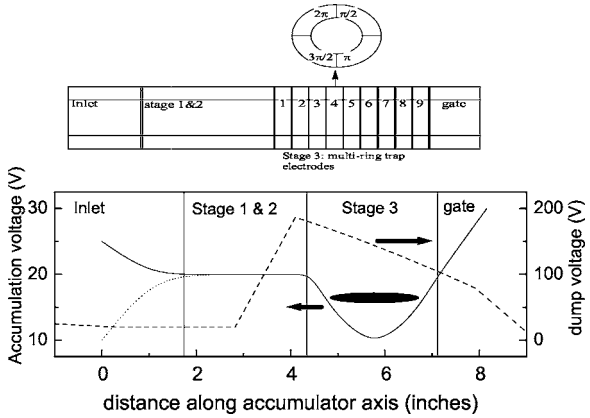

FIG. 5. Above: the accumulator electrode structure. The phases of the rf signal are indicated in the split ring. Below: the axial potential profiles for storing (solid line) and dumping (short dashed line) positron plasmas. The dotted line indicates the momentary (~100 ns) opening of the inlet to admit a pulse from the trap.

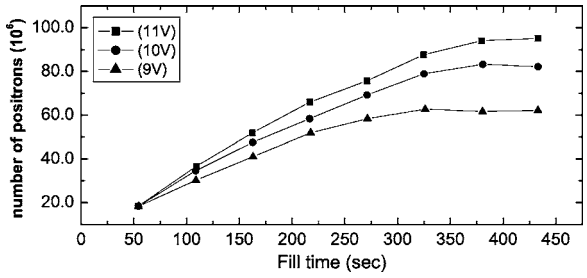

FIG. 6. A positron stacking curve in which the effect of lowering the well depth (indicated in the legend) increases the maximum number of positrons that can be stored.

well (stage 3), in which the positrons are accumulated from the trap with a subsidiary harmonic potential well, created using a multiring electrode trap.[33]

Positron pulses dumped from the trap are transferred to the accumulator by pulsing open the accumulator inlet electrode (see Fig. 5) with a suitable delay. The positrons are initially confined in stages 1–3 and then become trapped in the harmonic potential well in ~100 ms by collisions with gas atoms and other positrons. Since the transfer cycle is operated at 4 Hz, very few losses occur when the accumulator inlet potential is opened again to admit the next pulse.

The base pressure in the accumulator was 3×10^{-11} Torr which rose to 5×10^{-9} Torr due to buffer gas leakage from the trap. The lifetime against annihilation on nitrogen at this pressure is in excess of 1000 s.[34] However, the typical lifetime in the accumulator is only ~100 s due to anomalous cross-field transport.[29] In order to practically eliminate this loss mechanism, we employ the "rotating wall" technique as described in the literature.[30,31]

The action of the rotating wall on the plasma injects angular momentum, which not only counteracts outward transport but also produces a net reduction in plasma diameter. The compression produces significant heating of the plasma and so a cooling mechanism is required. Since the confining magnetic field in the accumulator was 500 G there was negligible cooling by cyclotron radiation. Thus a cooling gas (SF_6) was introduced at $\sim2\times10^{-8}$ Torr, at which pressure the annihilation rate is not significantly increased. At 2×10^{-8} Torr of SF_6 annihilation and cooling times of 2190 and 0.36 s have been measured, respectively.[34] Typical plasma temperatures for the compressed state were 0.1–0.2 eV, as measured by the method of Eggleston *et al.*[35]

Figure 6 is a stacking curve, which shows the accumulation of positrons as a function of time for various depths of the potential well. The saturation of these curves is primarily determined by the space charge potential of the plasmas, since clearly no further stacking is possible when this is equal to the confining electrode potential. The space charge potential (ϕ_{sp}) on the axis of an infinitely long plasma column with a uniform density is given by[36]

$$\phi_{sp} = 1.4\times10^{-7}\frac{N_p}{L}\left(1+2\ln\frac{r_w}{r_p}\right)\ (\mathrm{V}), \qquad (1)$$

where N_p is the total number of positrons, L is the plasma length in centimeters, r_p is the plasma radius, and r_w is the inner radius of the confining electrodes (1.27 cm). Although

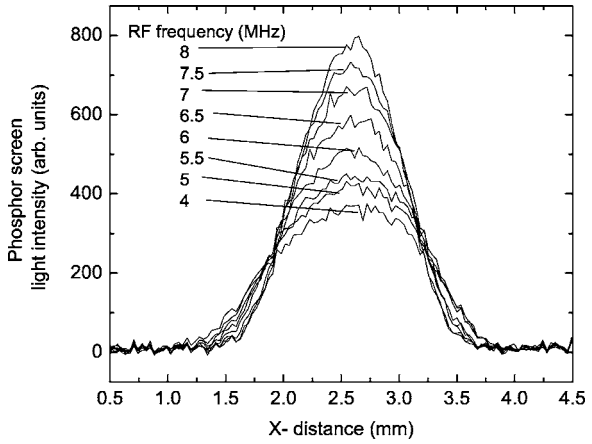

FIG. 7. Radial profiles of the positron plasma as a function of the applied rotating wall frequency, as measured by dumping the plasma onto phosphor screen biased to −5 kV and imaging it using a CCD camera. The plasmas shown in this figure contained around 2×10^7 positrons.

Eq. (1) is an approximation to the actual plasma configuration, the saturation of the stacking curves of Fig. 6 is consistent with the plasma space charge reaching the confining potential.

It has been found that optimal compression is obtained by accumulating the positrons with a RW frequency of ~4 MHz, (which is sufficient to counteract radial transport) and then increasing the frequency to ~8 MHz for a few seconds prior to dumping the plasma. We do not know exactly why this methodology seems to be more efficacious than using a fixed rf signal, but it seems likely that it has something to do with a reduction in plasma heating. Figure 7 shows the effect of using different frequencies during the final compression phase.

As is evident from Fig. 6, this methodology has allowed us to generate plasmas containing up to 95×10^6 positrons. We have observed very little variation in the areal density with the total number of positrons. The reason for this appears to be that the plasma density is limited by the frequency of the rf signal we are able to apply. Presently ~8 MHz is the highest frequency our generator is able to produce before disruptive phase shifting and nonlinear amplitude variations start to occur. A plasma rotation frequency of 8 MHz corresponds to a density of 2.7×10^8 cm^{-3} which would appear to be the density of our fully compressed plasmas.

Using these accumulation and compression techniques, we have been able to achieve areal densities up to 2×10^9 cm^{-2} once the plasma is dumped onto a planar target. As described in the next section, the density was further increased by the application of pulsed magnetic field at the target.

D. Spatiotemporal compression by pulsed electric and magnetic fields

It is well known that when a parabolic potential is rapidly applied to an ensemble of positrons they will arrive at the well minimum at the same time.[37] The positron plasmas are ejected from the accumulator by the application of an approximation to such a potential, as depicted in Fig. 5(b). A

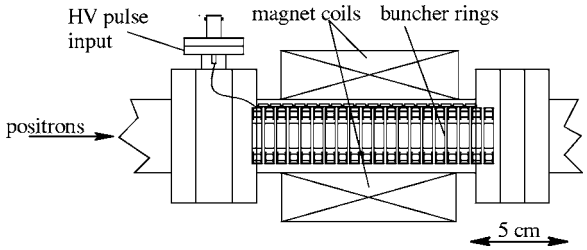

FIG. 8. The buncher layout. The bunching potential gradient was established by a string of resistors connecting neighboring accelerator rings with a total resistance of 50 Ω. Each resistor was formed from a short length of 100 Ω/ft resistance wire spot welded between two rings.

relatively small (200 V) pulse is used here which produces pulses with a temporal width that depends on the number of positrons in the pulse (or, more accurately, on the space charge potential of the positron plasma). This typically restricts the width to around 15–20 ns for plasmas containing over 1×10^6 positrons. In order to obtain subnanosecond pulses, a separate buncher was installed between the accumulator and the target region, which is depicted schematically in Fig. 8.

When the positron pulse enters the buncher a high voltage pulse (~50 ns long, variable up to 2 kV) is rapidly applied, with a rise time around 2 ns, which is short compared to the incoming positron pulse width. The resistors between the buncher rings are chosen so that the high voltage pulse creates a harmonic potential well along the length of the electrode structure.[37] This leads to subnanosecond pulses, as shown in Fig. 9. The time structure of the pulses was measured using a cylindrical 11×11 mm^2 PbF_2 crystal attached to a Hamamatsu R3809U-50 single stage microchannel plate photomultiplier. This photomultiplier has a single electron response time of ~250 ps, FWHM and since the PbF_2 crystal is a Cherenkov radiator[38] the light output is effectively instantaneous.

Typically, 2 kV pulses are used, which is sufficiently high with respect to the space charge potential of the plasma that the pulse width is independent of the number of positrons. Up to 70×10^6 positrons have been compressed into an ~1 ns pulse. Theoretically it should be possible to compress pulses to a width that depends on the square root of the ratio of the plasma energy spread to the applied high voltage pulse. However, we have found almost no improvement in increasing the high voltage pulse from 1 to 2 kV, implying

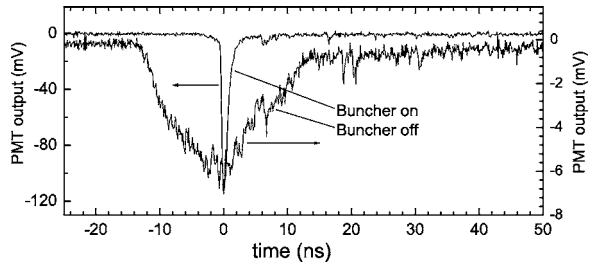

FIG. 9. The time width of the pulse with and without the buncher. The ~20 ns FWHM pulse emitted from the accumulator is compressed into a subnanosecond pulse with practically no loss of particles. The "buncher off" trace has been slightly displaced vertically for clarity.

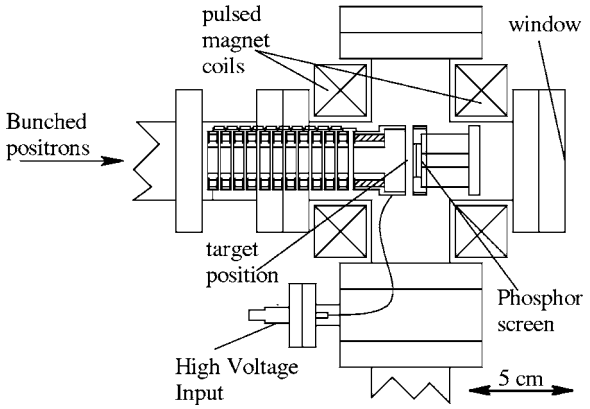

FIG. 10. The layout of the accelerator rings and the phosphor screen used to image the beam. The accelerator rings are interconnected in pairs by 1 MΩ KDI Pyrofilm vacuum compatible resistors and allow the beam to be accelerated up to 10 kV without the use of grids. The accelerator voltage is applied only for a short time to prevent overheating the resistors.

that some other unknown mechanism is limiting the time compression.

Positron plasmas typically have an areal density in the range of $(1-2)\times10^9$ cm^{-2} in the accumulator, which is too low for some of the high density positronium interactions we wish to study. For this reason the beam is further compressed at the target by a pulsed magnetic field of ~1 T. A schematic of the target chamber, accelerator rings, and magnet coils is shown in Fig. 10.

The pulsed magnetic field was generated using a capacitor bank consisting of twenty 15 mF 200 V aluminum electrolytic capacitors, switched using thyristors. This was able to generate a maximum current of 500 A per coil after charging for approximately 1 min, which is generally less than the positron fill time. A typical current pulse is shown in Fig. 11. The timing of the dump pulse from the accumulator was synchronized with the high voltage pulse to the buncher as well as the pulsed magnetic field to maximize the spatiotemporal pulse density.

This magnet generated a field of 1.25 T for a current of 500 A, but for typical operating conditions was generally closer to 1 T. The maximum positron areal density in the 500 G field of the accumulator was $\sim2\times10^9$ cm^{-2}. This was thus increased by a factor of 20 at the target due to the pulsed magnetic field at that location, producing areal densities in the range of $(2-4)\times10^{10}$ cm^{-2}. This has proved to be sufficiently high to observe positronium-positronium interactions for the first time.[16] The density of the beam was varied by

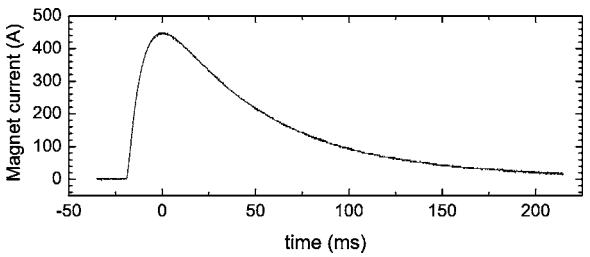

FIG. 11. The pulsed magnet current. The arrival of the positron pulse is tuned to coincide with the maximum magnetic field to maximize compression.

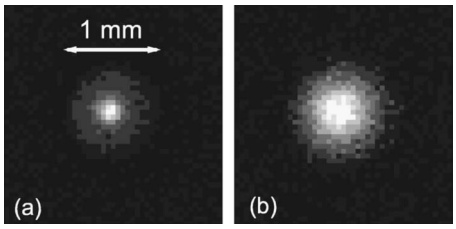

FIG. 12. The effect of the pulsed magnet on the beam compression. Image (a) is a fully compressed plasma with an areal density of around 3×10^{10} cm^{-2} while (b) has been allowed to expand for 3 s before being ejected from the accumulator, producing a beam with an areal density of 4.9×10^{9} cm^{-2}.

turning off the rotating wall for a variable period of time (0–3 s) prior to dumping. Figure 12 shows a fully compressed (a) and a reduced density (b) pulse imaged on the phosphor screen with a charge-coupled device (CCD) camera.

The beam impact energy was adjusted by using a multiring accelerator (see Fig. 10), which allowed distortion-free electrostatic acceleration without the need for any grids, thus avoiding positron losses and associated inconvenient gamma ray bursts. This also provided a convenient way to accelerate the beam to 5 kV or so, which was necessary for imaging using the phosphor screen. The screen was built into the end of the accelerator, and the target holder could be moved into the equipotential space just in front of the screen. This ensured that the beam size measured using the screen was very close to that on the target.

III. SINGLE SHOT LIFETIME MEASUREMENTS

The experiments we have conducted so far, as well as those planned for the future, utilize a new technique we have developed, which is a variation of positron annihilation lifetime spectroscopy (PALS).[39] Using a fast oscilloscope connected directly to the anode of a photomultiplier tube, we are able to record a lifetime spectrum in a single shot from the accumulator, and we refer to this as SSPALS.[40] This technique is very sensitive to the type of detector used since the complete detector response is folded into the lifetime spectra.

These bunching and compression techniques can be utilized in different combinations, depending on the particular experimental requirements. We now discuss two specific applications utilizing high spatial and temporal compressions, respectively.

A. Dense positronium gas

In this experiment positronium lifetimes of the order of 100 ns in a porous silica target were measured and so the ~20 ns pulses delivered directly from the accumulator were sufficient. Since the objective of this experiment was to observe dense positronium effects it was necessary to use the pulsed magnetic field and compress the beam spatially in order to achieve the required densities. For this work a 2×2 in.^{2} $PbWO_4$ scintillator attached to an XP2020 photomultiplier was used. This detector had an intrinsic time width of around 15 ns FWHM, and low afterglow, making it ideal for this experiment. This scintillator also has a low light output compared to most scintillators [approximately 1% of NaI(Tl)], but this is actually beneficial in this type of experiment since it helps prevent saturation of the photocathode following intense gamma ray bursts.

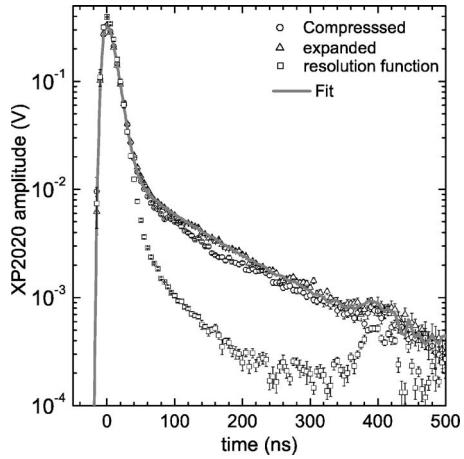

FIG. 13. Single shot lifetime spectra showing the effect of positronium-positronium interactions in porous silica. The resolution function is the system response, obtained using silicon and for which practically no positronium is formed. This was used as a Green's function in the fitting procedure. The areal densities of the beam were 3.3×10^{10} and 0.49×10^{10} cm^2 for the compressed and expanded cases, respectively. The feature at ~400 ns is an afterpulse caused by the ionization of residual gas in the photomultiplier tube (Ref. 43).

Figure 13 shows SSPALS data taken for three different cases; high and low areal densities with a porous silica target, and one high energy shot with a pure silicon target for reference. The latter was used as a system resolution function since the 7 kV beam is expected to produce very little ($<2\%$) positronium with this target. No difference was observed in this case for different beam densities. Conversely, a significant difference was observed for high and low densities in the porous silica, as is apparent from the figure. As described in more detail in Ref. 16, these differences can be attributed to Ps–Ps interactions.

B. Positron lifetime in Teflon

In another experiment a low-density, short-time pulse was used to measure the positronium lifetime in Teflon. In this case the buncher was used to produce an ~1 ns wide positron pulse (FWHM). For this measurement a 30 mm^2 $\times$20 mm long PbF_2 crystal, optically coupled to a Hamamatsu R2287U microchannel plate photomultiplier was used. This detector provided a response time of ~1.5 ns FWHM, including the positron pulse width (~1 ns FWHM). The same procedure described above was used to fit the data, although in this case the time resolution was sufficiently high that a pattern of high frequency oscillations can be discerned following the prompt peak at time $t=0$. These oscillations were reproducible from shot to shot if nothing in the experimental configuration was changed and proved to be caused by multiple reflections associated with slight variations in the characteristic impedance along the length of the ~10 m RG-8X cable connecting the photomultiplier anode to the oscilloscope. Different nominally identical cables, the same cable when reversed, and even a single cable after it had

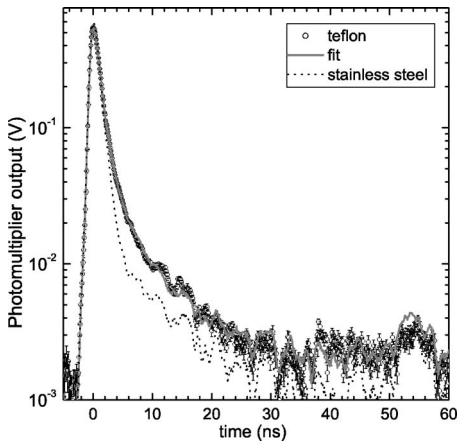

FIG. 14. Positronium lifetime spectrum in a Teflon sample using a PbF_2 crystal attached to an R2287U photomultiplier. The timing resolution is 1.55 ns FWHM and the pulse width is <1 ns. The small amplitude fine scale structure is due to small cable reflections. The feature at about 54 ns appears to be an ion after pulse similar to that observed in the XP2020 PMT.

been moved, all had distinct signatures of oscillations. This means that the resolution function had to be recorded in the same acquisition run as the actual data.

Figure 14 shows data taken with the Teflon sample as well as a resolution function, taken this time with a stainless steel target and was practically identical to one obtained with a silicon target. The best fit was obtained by including two positronium components; one with a lifetime of 2.8(0.1) ns and an intensity of 17(1)% and one with a lifetime of 94(5) ns and an intensity of 11(1)%. These values are in fair agreement with the 3.3–4.1 ns and 17%–26% reported in the literature[41–43] for various samples of Teflon at room temperature.

IV. DISCUSSION

We have described a device to create intense pulses of low energy positrons. With $\sim 60 \times 10^6$ positrons compressed to a width of 1 ns this amounts to an average positron current of 10 mA during the pulse. The use of a pulsed magnetic field in conjunction with the rotating wall compression has allowed us to create areal positron densities of 3×10^{10} cm^{-2}.

It is believed that the experiment to observe positronium molecules (Ps_2) will require subnanosecond pulses with areal densities of at least 1×10^{10} cm^{-2}.[20] These conditions have already been exceeded, and the required target preparation chamber is currently being installed. This experiment may involve additional methods not described in this article, such as laser excitation and ionization of the Ps_2 molecules.

The ability to provide such a large instantaneous positron density has made it possible for us to begin a new program of experimentation regarding dense positronium gases and transient phenomena in positronium forming materials. Although the primary motivation for these efforts has been the creation of a Bose-Einstein condensate of positronium,[19] the necessary steps towards this goal cannot help but yield many new methods and, more importantly, new physics.

ACKNOWLEDGMENTS

The authors gratefully acknowledge Dr. Maurizio Biasini for helpful comments. This work was supported in part by the National Science Foundation under Grant Nos. DMR 0216927 and PHY 0140382.

[1] P. A. M. Dirac, Proc. Cambridge Philos. Soc. **26**, 361 (1930).
[2] C. D. Anderson, Phys. Rev. **43**, 491 (1933).
[3] W. H. Cherry, Ph.D. thesis, Princeton University, Princeton, NJ, 1958, available from University Microfilms International, Ann Arbor, MI.
[4] D. E. Groce, D. G. Costello, J. W. McGowan, and D. F. Herring, Bull. Am. Phys. Soc. **13**, 1397 (1972).
[5] K. F. Canter, P. G. Coleman, T. C. Griffith, and G. R. Heyland, J. Phys. B **5**, L167 (1972).
[6] A. P. Mills, Jr., in *Positron Solid State Physics*, edited by A. Dupasquier and W. Brandt (North-Holland, Amsterdam, 1983), p. 432.
[7] See *Positron Beams and Their Applications*, edited by P. G. Coleman (World Scientific, Singapore, 2000).
[8] K. G. Lynn, A. P. Mills, Jr., R. N. West, S. Berko, K. F. Canter, and L. O. Roellig, Phys. Rev. Lett. **54**, 1702 (1985); C. Hugenschmidt, G. Kogel, R. Repper, K. Schreckenbach, P. Sperr, B. Strasser, and W. Triftshauser, Nucl. Instrum. Methods Phys. Res. B **192**, 97 (2002); A. van Veen, H. Schut, F. Labohm, and J. de Roode, Nucl. Instrum. Methods Phys. Res. A **427**, 266 (1999).
[9] W. E. Kauppila, T. S. Stein, and G. Jesion, Phys. Rev. Lett. **36**, 580 (1976); R. Xie, M. Petkov, D. Becker, K. Canter, F. M. Jacobsen, K. G. Lynn, R. Mills, and L. O. Roellig, Nucl. Instrum. Methods Phys. Res. B **93**, 98 (1994); D. B. Cassidy, K. F. Canter, R. E. Shefer, R. E. Klinkowstein, and B. J. Hughey, *ibid.* **195**, 442 (2002).
[10] R. H. Howell, I. J. Rosenberg, and M. J. Fluss, Appl. Phys. A: Solids Surf. **43**, 247 (1987).
[11] S. Okada and H. Sunaga, Nucl. Instrum. Methods Phys. Res. B **56–57**, 604 (1991).
[12] There are, however, some experiments that are simply not possible with low intensity beams. For example, see D. B. Cassidy *et al.*, Phys. Rev. C **64**, 054603 (2001).
[13] To our knowledge encapsulated sources suitable for use in positron beams are now only available from a single commercial supplier, http://www.tlabs.ac.za/public/Radioisotopes.htm
[14] C. M. Surko and R. G. Greaves, Phys. Plasmas **11**, 2333 (2004).
[15] S. J. Gilbert, C. Kurz, R. G. Greaves, and C. M. Surko, Appl. Phys. Lett. **70**, 1944 (1997).
[16] D. B. Cassidy, S. H. M. Deng, R. G. Greaves, T. Maruo, N. Nishiyama, J. B. Snyder, H. K. M. Tanaka, and A. P. Mills, Jr., Phys. Rev. Lett. **95**, 195006 (2005).
[17] ATHENA Collaboration, M. Amoretti *et al.*, Nature (London) **419**, 456 (2002); G. Gabrielse *et al.*, Phys. Rev. Lett. **89**, 213401 (2002).
[18] C. M. Surko, G. F. Gribakin, and S. J. Buckman, J. Phys. B **38**, R57 (2005).
[19] P. M. Platzman and A. P. Mills, Jr., Phys. Rev. B **49**, 454 (1994).
[20] A. P. Mills, Jr., Nucl. Instrum. Methods Phys. Res. B **192**, 107 (2002).
[21] D. B. Cassidy *et al.* (unpublished).
[22] D. B. Cassidy and J. A. Golovchenko in *New Directions in Antimatter Chemistry and Physics*, edited by C. M. Surko and F. A. Gianturco (Kluwer, Dordrecht, 2001), p. 83.
[23] T. J. Murphy and C. M. Surko, Phys. Rev. A **46**, 5696 (1992).
[24] R. G. Greaves and J. Moxom, AIP Conf. Proc. **692**, 140 (2003).
[25] K. Iwata, R. G. Greaves, T. J. Murphy, M. D. Tinkle, and C. M. Surko, Phys. Rev. A **51**, 473 (1995).
[26] A. P. Mills, Jr. and E. M. Gullikson, Appl. Phys. Lett. **49**, 1121 (1986).
[27] ATHENA Collaboration, L. V. Jørgensen *et al.*, Phys. Rev. Lett. **95**, 025002 (2005).
[28] J. P. Sullivan, J. P. Marler, S. J. Gilbert, S. J. Buckman, and C. M. Surko, Phys. Rev. Lett. **87**, 073201 (2001).
[29] J. H. Malmberg and C. F. Driscoll, Phys. Rev. Lett. **44**, 654 (1980).
[30] F. Anderegg, E. M. Hollmann, and C. F. Driscoll, Phys. Rev. Lett. **81**, 4875 (1998).
[31] R. G. Greaves and C. M. Surko, Phys. Rev. Lett. **85**, 1883 (2000).
[32] J. Clarke, D. P. van der Werf, B. Griffiths, D. C. S. Beddows, M. Charlton, H. H. Telle, and P. R. Watkeys Rev. Sci. Instrum. **77**, 063302 (2002); J. Sullivan, personal communication.
[33] H. Higaki and A. Mohri, Jpn. J. Appl. Phys., Part 1 **36**, 5300 (1997); A.

Mohri, *ibid.* **37**, 664 (1998).
[34] R. G. Greaves and C. M. Surko, Phys. Plasmas **8**, 1879 (2001).
[35] D. L. Eggleston, C. F. Driscoll, B. R. Beck, A. W. Hyatt, and J. H. Malmberg, Phys. Fluids B **4**, 3432 (1992).
[36] R. C. Davidson, *Physics of Nonneutral Plasmas* (Addison-Wesley, Reading, MA, 1990).
[37] A. P. Mills, Jr., Appl. Phys. **22** 273 (1980).
[38] D. F. Anderson, M. Kobayashi, C. L. Woody, and Y. Yoshimura, Nucl. Instrum. Methods Phys. Res. A **290**, 385 (1990).
[39] See, e.g., I. K. Mackenzie, *Positron Solid State Physics*, Proceedings of the International School of Physics "Enrico Fermi," Course 83, edited by W. Brandt and A. Dupasquier (North-Holland, Amsterdam, 1983), p. 196.
[40] D. B. Cassidy, S. H. M. Deng, H. K. M. Tanaka, and A. P. Mills, Jr., Appl. Phys. Lett. **88**, 194105 (2006).
[41] W. Brandt and I. Spirn, Phys. Rev. **142**, 231 (1965).
[42] M. N. G. Khan, D. J. Carswell, and J. Bell, Br. J. Appl. Phys., J. Phys. D **1**, 1833 (1968).
[43] M. Bertolaccini, A. Bisi, G. Gambarini, and L. Zappa, J. Phys. C **7**, 3827 (1974).